JOURNAL OF WAVE-MATERIAL INTERACTION
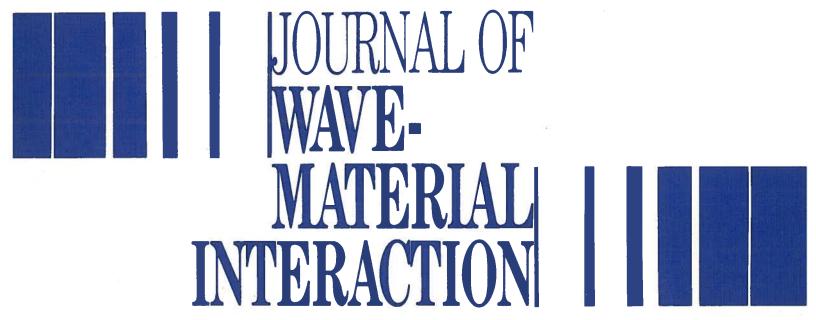
GEOMETRY CAN BE THE BASIS FOR ACOUSTIC ACTIVITY

(*A LA* OPTICAL ACTIVITY) IN COMPOSITE MEDIA

VASUNDARA V. VARADAN, AKHLESH LAKHTAKIA and VIJAY K. VARADAN
Laboratory for Electromagnetic and Acoustic Research,
Department of Engineering Science & Mechanics,
and
The Center for the Engineering of Electronic and Acoustic Materials,
The Pennsylvania State University,
University Park, PA 16802.

ABSTRACT

Optical activity is exhibited by media whose molecular configurations are handed or chiral. Since geometry is the basis for chirality, it can be probed by transverse waves, but not by longitudinal waves. Therefore, solid composite media can also be chiral because the acoustic fields in solid media consist, in general, of both transverse and longitudinal components. To explore this conjecture, the acoustically active medium is modeled by beaded helices embedded in a matrix material. The helix is comprised of tiny rigid spheres strung along a helical strand which is indistinguishable from the matrix medium. The field scattered by a beaded helix is computed by modeling the individual spheres as point dipoles, with multiple scattering theory being used to account for the dipole-dipole interactions. The computed results justify the premise of this communication.

1. INTRODUCTION

Many organic molecules occur as stereoisomers in enantiomorphic pairs, i.e., one isomer is the mirror image of the other one, but the two of them are not congruent with each other. These mirror-conjugates possess different physical properties even though their molecular formulae are identical [1]. The basis for the difference in the physical properties of the mirror-conjugates lies in the handedness or the chirality possessed by their molecular configurations. Thus, it is well-known that when an electromagnetic disturbance travels through a medium consisting of chiral molecules, it is forced to adapt to the handedness of the molecules. In other words, linearly polarized planewaves cannot be made to propagate through such a medium; whereas left- and right-circularly polarized planewaves, travelling with different phase velocities, are perfectly acceptable solutions of the vector wave equation for this class of media [2].

Electromagnetic waves can recognize the handedness of a chiral object primarily due to their transverse nature, i.e., the applicable vector infinite medium Green's function recognizes the vector distance between the field point and the source point. Longitudinal fields, such as acoustic waves in fluids, cannot do so because the pertinent Green's function is purely scalar. However, acoustic fields in solids have both longitudinal and transverse components [3]. There is every reason to believe, therefore, that solid media can be endowed with "acoustic" activity *a la* optical activity [1,2]. Thus, an acoustically active medium may be constructed by embedding macroscopic chiral objects, all of the same handedness, in a host medium; the resulting effective medium should then exhibit chirality. By varying the concentrations and the sizes of the chiral inclusions, the properties of the composite medium may be altered to suit desired characteristics. In view of the flourishing research efforts being bestowed on novel polymers and composites, it is possible that acoustically active media may turn out to be of considerable importance.

With this motivation, we have decided here to explore if the inclusion geometry can serve as a basis for acoustical activity in composite solids. The chiral objects used here consist of tiny rigid spheres suspended on a helical strand which is indistinguishable from the surrounding space [4]. Whereas each bead is sufficiently small to be modeled as the equivalent of a point electric dipole, the overall size of the finite helical arrangement can be large enough to be in the high-frequency regime. From the computed results, it is deduced

that the geometrical arrngement of inclusions in a matrix medium can be exploited to construct acoustically active composite media.

2. RAYLEIGH SCATTERING BY A RIGID SPHERE

The primary component of the present investigation is the acoustic response of a tiny rigid sphere, it being our contention that such a scatterer can be modeled as a point dipole, exactly as in the electromagnetic case. Consider, therefore, a small rigid sphere of radius b embedded in a host medium of density ρ and Lame constants λ and μ. On this sphere, there is a field incident whose displacement vector is u_{inc}, and as a result of which a surface traction t_+ is induced [5]. This surface traction then re-radiates creating the scattered field u_{sc} given by

$$u_{sc}(r) = - \iint_S d^2r_0 \; \mathcal{G}(r,r_0) \cdot t_+(r_0), \quad r \text{ outside } S \tag{1}$$

as per Huyghens' principle [6]. In (1), the Green's dyadic can be resolved into longitudinal (p) and transverse (s) components as [3,6]

$$\mathcal{G}(r,r_0) = \mathcal{G}_p(r,r_0) + \mathcal{G}_s(r,r_0), \tag{2a}$$

$$\mathcal{G}_p(r,r_0) = - (k_p^3/\rho\omega^2)[k_p^{-2}\nabla\nabla]g(k_pR)/4\pi, \tag{2b}$$

$$\mathcal{G}_s(r,r_0) = (k_s^3/\rho\omega^2)[\mathcal{I} + k_s^{-2}\nabla\nabla]g(k_sR)/4\pi, \tag{2c}$$

in which $\mathcal{I}$ is the identity dyadic, $R = r - r_0$ and $g(\xi) = \exp[i\xi]/\xi$. An $\exp[-i\omega t]$ harmonic time-dependence will be implicit throughout this paper; $k_p^2 = \omega^2\rho/[\lambda+2\mu]$ and $k_s^2 = \omega^2\rho/\mu$.

In the far zone, i.e. for $k_p r \gg 1$ and $k_s r \gg 1$, $\mathcal{G}_s(r,r_0)$ is purely transverse and $g(kR)$ can be approximated by $g(kr)\exp[-ike_r \cdot r_0]$ as per Kleinman and Senior [7], e_r being the radial vector in the spherical co-ordinate system. Furthermore, the sphere is tiny, i.e., $k_p b \ll 1$ and $k_s b \ll 1$, which implies that $g(kR)$ can be adequately approximated by $g(kr)$ [7]. Thus, it is possible to restate (1) in the form

$$u_{sc}(r) = \mathcal{D}(r) \cdot \Pi, \tag{3a}$$

where the dyadic $\mathcal{D}(r)$ is given by

$$\mathcal{D}(r) = g(k_p r) e_r e_r \cdot \mathcal{I} - (k_s/k_p)^3 g(k_s r) e_r \times e_r \times \mathcal{I}, \tag{3b}$$

the *equivalent* dipole moment being

$$\Pi = (-1/4\pi) (k_p^3/\rho\omega^2) \iint_S d^2r_0 \; t_+(r_0). \tag{3c}$$

It follows from (3) that the replacement of a small rigid sphere by an equivalent dipole moment is a well-founded concept.

For a small sphere, the dipole moment Π can be easily derived by heuristic means without resorting to (3c). If a longitudinal wave $u_{inc} = e_z \exp[ik_p z]$ were to be incident on the rigid sphere, then in the Rayleigh limit it has been shown by Knopoff [8] that the scattered field in the far zone will be

$$u_{sc}(r) = \alpha \; \mathcal{D}(r) \cdot e_z; \quad \alpha = 3k_p b \, [1 + 2 \, (k_s/k_p)^2]^{-1}. \tag{4a,b}$$

while the scattered displacement corresponding to an incident shear wave $u_{inc} = e_x \exp[ik_s z]$ in the same circumstances will be [9]

$$u_{sc}(r) = \alpha \; \mathcal{D}(r) \cdot e_x. \tag{4c}$$

Without loss of generality, then it is possible to state that α is the equivalent polarizability of a rigid sphere, and

$$\mathbf{u}_{sc}(\mathbf{r}) = \mathbb{D}(\mathbf{r}) \cdot \Pi = \alpha \, \mathbb{D}(\mathbf{r}) \cdot \mathbf{u}_{inc} \tag{5}$$

in the far zone.

3. FIELD SCATTERED BY A BEADED HELIX

The helix on which the rigid spheres are located is given, in a cartesian co-ordinate system, by the radius vector

$$\mathbf{r}(\zeta) = a[\mathbf{e}_x \cos\zeta + \mathbf{e}_y \, h \sin\zeta] + \mathbf{e}_z \, P(\zeta/2\pi), \quad \zeta \in \{-\infty, \infty\}, \tag{6}$$

where a is the radius and P is the pitch of the helix; the handedness parameter h = +1 if the helix curls up in the +z direction according to the right-handed rule, and h = -1, if otherwise. The identical spheres are arranged on this helical coil as follows: Let the helix be finite in extent, having 2N+1 complete rotations so that ζ extends over the range $\{-(2N+1)\pi, (2N+1)\pi\}$, N being a positive integer or zero. On each of the 2N+1 rings of this finite helix, there are 2M+1 beads arranged over equal–$\Delta\zeta$ segments, M being an integer greater than zero. Then, the position vector of the mth bead on the helix is given as

$$\mathbf{r}_m = a[\mathbf{e}_x \cos\zeta_m + \mathbf{e}_y \, h \sin\zeta_m] + \mathbf{e}_z \, P(\zeta_m/2\pi), \quad m \in \{1,Q\}, \tag{7a}$$

where,

$$\zeta_m = \pi(2m-Q-1)/(2M+1), \quad Q = (2N+1)(2M+1). \tag{7b,c}$$

Each of the Q spheres in this arrangement has a radius b which is small enough that no two of them ever touch; the condition $2(2M+1)b \le \min\{a,P\}$ shall definitely guarantee that.

Consider that a displacement field $\mathbf{u}_{inc}$ is incident on this helical arrangement; it can be any arbitrary field so long as its source is not located anywhere inside or on the minimum sphere circumscribing the helix. But this is not the actual field $\mathbf{U}_m$ which excites the mth sphere. It is easy to see that the field exciting the mth bead can be self-consistently written as [10]

$$\mathbf{U}_m = \mathbf{u}_{inc}(\mathbf{r}_m) + \sum_{n,n\ne m} \mathbf{u}_{rad,n}(\mathbf{r}_m), \tag{8}$$

in which $\mathbf{u}_{rad,n}$ is the radiated (i.e., scattered) displacement due to the nth equivalent dipole (i.e., sphere) evaluated at the location of the mth sphere. Mathematically [6,7],

$$\mathbf{u}_{rad,n}(\mathbf{r}) = (4\pi\rho\omega^2/k_p^3)\mathbb{G}(\mathbf{r}, \mathbf{r}_n) \cdot \Pi_n = \alpha \, (4\pi\rho\omega^2/k_p^3)\mathbb{G}(\mathbf{r}, \mathbf{r}_n) \cdot \mathbf{U}_n. \tag{9}$$

Equations (8) and (9) can be combined to yield

$$\mathbf{U}_m - \alpha \, (4\pi\rho\omega^2/k_p^3) \sum_{n,n\ne m} [\mathbb{G}(\mathbf{r}_m, \mathbf{r}_n) \cdot \mathbf{U}_n] = \mathbf{u}_{inc}(\mathbf{r}_m), \tag{10}$$

which can be solved for the exciting fields $\mathbf{U}_m \; \forall m \in \{1,Q\}$.

Once the solution of (10) has been obtained, the total scattered field outside the circumscribing sphere can be computed simply as [10]

$$\mathbf{u}_{sc}(\mathbf{r}) = \alpha \, (4\pi\rho\omega^2/k_p^3) \sum_m \mathbb{G}(\mathbf{r}, \mathbf{r}_m) \cdot \mathbf{U}_m. \tag{11}$$

which, for $k_p r \to \infty$ and $k_s r \to \infty$, can be simplified to

$$u_{sc}(r) = g(k_p r) S_r(r) e_r + g(k_s r) [S_\theta(r) e_\theta + S_\varphi(r) e_\varphi],$$ (12)

in which the form functions are given as

$$S_r(r) = \alpha \sum_m \exp[-ik_p e_r \cdot r_m] e_r \cdot U_m,$$ (13a)

$$S_\theta(r) = \alpha (k_s/k_p)^3 \sum_m \exp[-ik_s e_r \cdot r_m] e_\theta \cdot U_m,$$ (13b)

$$S_\varphi(r) = \alpha (k_s/k_p)^3 \sum_m \exp[-ik_s e_r \cdot r_m] e_\varphi \cdot U_m.$$ (13c)

It is again emphasized here that, in deriving (10) and (12), there are no restrictions placed either on the radius a or on the pitch P of the helix; the only limitation here is that the radius b of each of the beads be sufficiently small so that its scattering response can be adequately described *via* (5).

4. NUMERICAL RESULTS AND DISCUSSION

Equations (10) and (12) were programmed on a DEC VAX 11/730 minicomputer and the exciting fields U_m as well as the form functions S_r, etc. were computed for computed longitudinal ($u_{inc} = e_z \exp[ik_p z]$) and transverse ($u_{inc} = e_x \exp[ik_s z]$) plane waves moving in the +z direction. This particular configuration for the incident fields was chosen to maximize the effect of chirality on the scattered fields.

Multiple scattering between the spheres would ensure that $U_m \neq u_{inc}(r_m)$. It is to be expected that the exciting fields should reflect the chirality of the helical arrangement of the rigid spheres. This, indeed turned out to be the case. For the two cases of the incident fields mentioned, it was observed that the y-directed component of U_m reversed its sign if the handedness parameter h changed its sign too. This virtually guarantees the fact that the acoustic waves in an elastic solid can recognize the chirality of an inclusion.

Further proof of this assertion is afforded by Figs. 1 and 2, in which the magnitudes and the phases of the form functions S_r, S_θ and S_φ are plotted against φ in the equatorial plane $\theta = \pi/2$ when a shear wave $u_{inc} = e_x \exp[ik_s z]$ is incident on a 9-sphere arrangement; N = M = 1, $k_p a = 1.0$, P/a = 3.0, $k_s/k_p = 3.0$, and $k_p b = 0.033$. For Fig. 1, the helix is right-handed (h = +1), while in Fig. 2 h = -1. There is no straightforward procedure to make the plots of Fig. 1 congruent with those of Fig. 2, although they look very similar: indeed, all of the magnitude plots of Fig. 1 are congruent with the respective mirror images of the magnitude plots of Fig. 2, and two of the three phase plots also exhibit similar congruences.
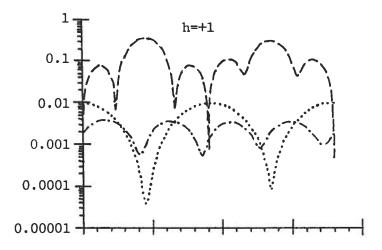
Reinforcement of the fact that geometry can be the basis of acoustical activity comes also from Fig. 3, in which the computations of Figs. 1 and 2 are combined but for the incident longitudinal wave, $u_{inc} = e_z \exp[ik_p z]$. Although the incident wave in this case is longitudinal, acoustic activity is manifested because each sphere radiates both longitudinal and transverse waves as per (5).

Finally, it is common knowledge that the scattered field can be expanded in terms of the vector mutipoles as

$$u_{sc}(r) = \Sigma_{\sigma mn} [A_{\sigma mn} L_{\sigma mn}^{(3)}(k_p r) + B_{\sigma mn} M_{\sigma mn}^{(3)}(k_s r) + C_{\sigma mn} N_{\sigma mn}^{(3)}(k_s r)],$$ (14)

in which L, M and N are the vector multipoles or spherical wave functions [3] and A, B and C are the multipole coefficients of expansions. Using the asymptotic expansions of the vector wave functions in the far zone along with the form functions, the multipole coefficients can be computed (see Appendix). For the computed results of Figs. 1–3, the ten lowest order multipole coefficients are tabulated in Table 1. Although the magnitudes of the multipole coefficients are the same for h = ± 1, it is clear that their phases cannot be made to coincide for right- and left- handed helices.

In conclusion, it has been shown here that the geometrical arrangement of inclusions in a matrix material can be exploited to yield acoustically active composite media. It is not necessary for the inclusions to
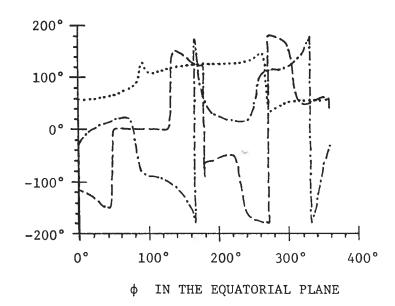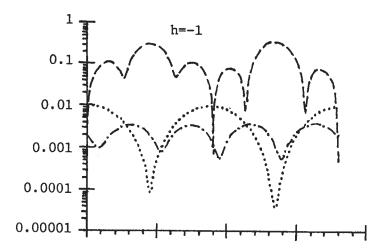
Figure 1 Computed values of the magnitudes and the phases of the form functions $S_r(\pi/2,\varphi)$ [• • • •], $S_\theta(\pi/2,\varphi)$ [−•−•−•−] and $S_\varphi(\pi/2,\varphi)$ [− − − −] for a right-handed helical arrangement (h = +1) of small rigid spheres, on which a shear wave $u_{inc} = e_x \exp[ik_s z]$ is incident. For the matrix material, $k_s/k_p = 3.0$. The helical arrangement is comprised of 9 spheres of radius b arranged on a 3-ring helix (M=N=1); $k_p b = 0.033$ so that the polarizability $\alpha = 0.5263\times10^{-2}$. The normalized helix radius $k_p a = 1.0$, and the normalized pitch $k_p P = 3.0$.

Figure 2 Same as Fig. 1, except h = -1.

ϕ IN THE EQUATORIAL PLANE

Figure 3 Computed values of the magnitudes and the phases of the form functions $S_r(\pi/2, \varphi)$ [• • •], $S_\theta(\pi/2, \varphi)$ [– • – • – •] and $S_\varphi(\pi/2, \varphi)$ [– – – –] for right- (h=+1) and left- (h=$\bar{1}$) handed helical arrangements of small rigid spheres, on which a longitudinal wave $\mathbf{u}_{inc} = \mathbf{e}_z \exp[ik_p z]$ is incident. For the matrix material, $k_s/k_p = 3.0$. The helical arrangement is comprised of 9 spheres of radius b arranged on a 3-ring helix (M=N=1); $k_p b = 0.033$ so that the polarizability $\alpha = 0.5263\times10^{-2}$. The normalized helix radius $k_p a = 1.0$, and the normalized pitch $k_p P = 3.0$.
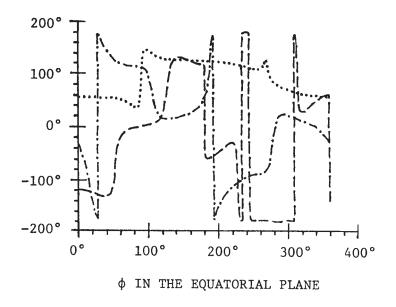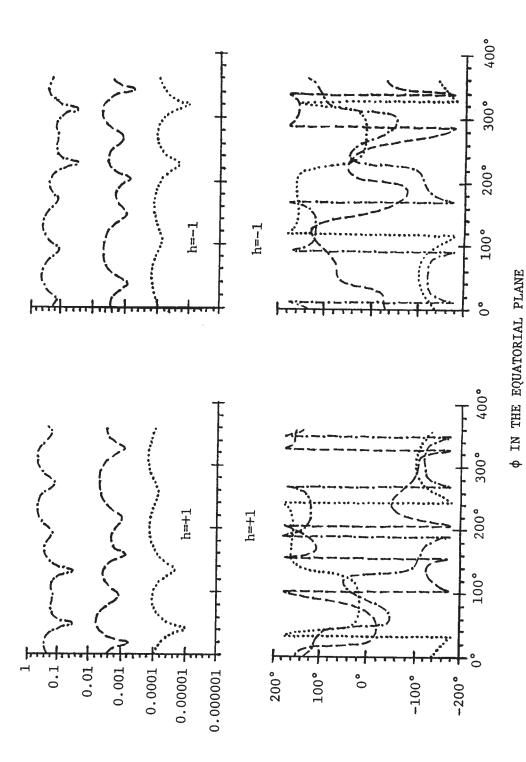
be rigid spheres; they can have different constitution and shape. Further work in this area is being carried on by us and will be reported in the near future.

TABLE I

Computed values of the multipole coefficients for right- and left-handed helical arrangements of small rigid spheres. For the matrix material, $k_s/k_p = 3.0$. The helical arrangement is comprised of 9 spheres of radius b arranged on a 3-ring helix (M = N = 1); $k_p b = 0.033$ so that the polarizability $\alpha = 0.5263 \times 10^{-2}$. The normalized helix radius $k_p a = 1.0$, and the normalized pitch $k_p P = 3.0$.

multipole coefficients	$u_{inc} = e_z \exp[ik_p z]$			$u_{inc} = e_x \exp[ik_s z]$		
	magnitude	phase (h = +1)	phase (h = -1)	magnitude	phase (h = +1)	phase (h = -1)
A_{e00}	1.1448	−0.097°	−0.097°	0.2018	−81.978°	−81.978°
A_{e01}	3.5777	89.809°	89.809°	0.3722	34.503°	34.503°
A_{e11}	0.3713	17.896°	17.896°	0.0957	−91.297°	−91.297°
A_{o11}	0.3103	−90.579°	89.421°	0.0437	−171.249°	8.751°
B_{e01}	0.0067	−58.447°	121.553°	0.0060	−51.338°	128.663°
B_{e11}	0.2644	158.683°	−13.169°	0.0035	137.088°	−42.912°
B_{o11}	0.3405	−90.054°	−90.054°	0.3453	−178.046°	−178.046°
C_{e01}	0.1423	−113.879°	113.879°	0.1612	−178.346°	178.346°
C_{e11}	0.0917	176.209°	−176.209°	0.4570	171.939°	−171.939°
C_{o11}	0.1283	−90.166°	−89.834°	0.0035	−75.837°	−104.162°

APPENDIX

The ten lowest order multipole coefficients of the field scattered by the helix can be computed as follows:

$$A_{e00} = (1/4\pi) \int_0^\pi d\theta \sin\theta \int_0^{2\pi} d\varphi \, [S_r(\theta,\varphi)],$$

$$A_{e01} = (3i/4\pi) \int_0^\pi d\theta \sin\theta \int_0^{2\pi} d\varphi \, [S_r(\theta,\varphi) \cos\theta],$$

$$A_{e11} = (3i/2\pi) \int_0^\pi d\theta \sin\theta \int_0^{2\pi} d\varphi \, [S_r(\theta,\varphi) \sin\theta \cos\varphi],$$

$$A_{o11} = (3i/2\pi) \int_0^\pi d\theta \sin\theta \int_0^{2\pi} d\varphi \, [S_r(\theta,\varphi) \sin\theta \sin\varphi],$$

$$B_{e01} = (-3/4\pi) \int_0^\pi d\theta \sin\theta \int_0^{2\pi} d\varphi \, [S_\varphi(\theta,\varphi) \sin\theta],$$

$$B_{e11} = (3/8\pi) \int_0^\pi d\theta \sin\theta \int_0^{2\pi} d\varphi \, [S_\theta(\theta,\varphi) \sin\varphi + S_\varphi(\theta,\varphi) \cos\theta \cos\varphi],$$

$$B_{o11} = (3/8\pi) \int_0^\pi d\theta \sin\theta \int_0^{2\pi} d\varphi \, [-S_\theta(\theta,\varphi) \cos\varphi + S_\varphi(\theta,\varphi) \cos\theta \sin\varphi],$$

$$C_{e01} = (-3i/4\pi) \int_0^\pi d\theta \sin\theta \int_0^{2\pi} d\varphi \, [S_\theta(\theta,\varphi) \sin\theta],$$

$$C_{e11} = (-3i/8\pi) \int_0^\pi d\theta \sin\theta \int_0^{2\pi} d\varphi \, [S_\theta(\theta,\varphi) \cos\theta \cos\varphi + S_\varphi(\theta,\varphi) \sin\varphi],$$

$$C_{o11} = (-3i/8\pi) \int_0^\pi d\theta \sin\theta \int_0^{2\pi} d\varphi \, [S_\theta(\theta,\varphi) \cos\theta \sin\varphi - S_\varphi(\theta,\varphi) \cos\varphi].$$

REFERENCES

1. A. Lakhtakia, V.V. Varadan and V.K. Varadan, "A parametric study of microwave reflection characteristics of a planar achiral-chiral interface," *IEEE Trans. Electromagn. Compat.* **EMC-25**, 90-95 (1986).

2. A. Lakhtakia, V.K. Varadan and V.V. Varadan, "Scattering and absorption characteristics of lossy dielectric, chiral, nonspherical objects," *Appl. Opt.* **24**, 4146-4154 (1985).

3. P.M. Morse and H. Feshbach, *Methods of Theoretical Physics II*, McGraw-Hill, New York (1953).

4. C.W. Patterson, S.B. Singham, G.C. Salzman and C. Bustamente, "Circular intensity differential scattering of light by hierarchial molecular structures," *J. Chem. Phys.* **84**, 1916-1921 (1986).

5. V.V. Varadan, "Elastic wave scattering," in *Acoustic, Electromagnetic and Elastic Wave Scattering* (V.K. Varadan and V.V. Varadan, Eds.), Pergamon, New York (1980).

6. Y.-H. Pao and V. Varatharajulu, "Huyghens' principle, radiation condition, and integral formulas for the scattering of elastic waves," *J. Acoust. Soc. Am.* **59**, 1361-1371 (1976).

7. R.E. Kleinman and T.B.A. Senior, "Rayleigh scattering," in *Low and High Frequency Asymptotics* (V.K. and V.V. Varadan, Eds.), North-Holland, Amsterdam (1986).

8. L. Knopoff, "Scattering of compression waves by spherical obstacles," *Geophys.* **24**, 30-39 (1959). [The two formulae 25 of this paper contain the same error: the factor a/r should be replaced by a/pr.]

9. L. Knopoff, "Scattering of shear waves by spherical obstacles," *Geophys.* **24**, 209-219 (1959). [Formula 38 of this paper contains an error: in the θ-directed component of U^S, $\sin\theta$ should be replaced by $\cos\theta$.]

10. V.K. Varadan, "Multiple scattering of acoustic, electromagnetic and elastic waves," in *Acoustic, Electromagnetic and Elastic Wave Scattering* (V.K. and V.V. Varadan, Eds.), Pergamon, New York (1980).